ifications. For the analysis of tetramer staining at equilibrium, T cells were stained for 2 h at room temperature with 20 μl of wash medium (0.2% sodium bicarbonate, 0.1% sodium azide and 2% FBS in RPMI-1640) containing anti-CD8α-FITC (clone YTS169.4; 0.5 μg) and different concentrations of tetramers (8.55, 17.1, 42.75 and 85.5 nM). Titration studies with 8.3-TCRαβ-transgenic $CD8^+$ T cells indicated that tetramer staining in the presence of this anti-CD8 monoclonal antibody does not change the percentage or absolute number of cells that bind the tetramer. After washing, cells were resuspended in 100 μl of wash medium and analysed with a flow cytometer.

The apparent K_d values were determined by plotting the negative reciprocal of the slope of the line fit to Scatchard plots of fluorescence units (median of $CD8^+$ population staining for tetramer) divided by concentration (nM) versus fluorescence units. For the analysis of binding half-life, T cells were stained with 85.5 nM tetramer and 0.5 μg of anti-CD8-FITC in 20 μl of wash medium for 45 min at room temperature. Cells were washed three times, cooled to 4 °C and resuspended in 100 μl of cold medium containing 50 μg of an anti-K^d monoclonal antibody (20-8-4S) or no antibody at all (negative control). Aliquots of 20 μl were taken at 0, 30, 60 and 90 min, diluted in 200 μl of wash medium and analysed with a flow cytometer. Half-lives ($t_{1/2}$) were determined by calculating the (ln 2)/mean slope value of plots of the corrected natural logarithm (ln) of the percentage normalized fluorescence (sum of fluorescence intensities of tetramer-positive $CD8^+$ T cells normalized per $CD8^+$ T cell at each point with respect to the initial time point) versus time. Studies of binding decay using samples from 9-week-old NOD mice indicated that half-lives calculated from 0–120-min slopes were not statistically different from the half-life values calculated from 0–90-min slopes ($n = 6$; 138 ± 17 versus 165 ± 24 min, respectively). The 120-min analysis was therefore omitted from studies at older ages, to overcome limitations in cell numbers.

^{51}Cr-release assays

Cytotoxicity assays were done as described[2], using peptide-pulsed (1 μg ml^{-1}) RMA-S-K^d cells labelled with [^{51}Cr]sodium chromate as targets at a 1:10 target:effector ratio.

Peptide treatment

Three week-old female NOD mice were injected with 100 μg of peptide in PBS intraperitoneally (i.p.) or through the footpad (f.p.). This was done every 2 weeks until week 7, and every 3 weeks thereafter. Mice were monitored for development of hyperglycaemia until week 32.

Pathology

Formalin-fixed, paraffin-embedded pancreas sections were stained with haematoxylin and eosin and scored for insulitis as described[8].

Statistical analyses

Data were compared using linear regression and variance analysis, Mann–Whitney U test or χ^2 test.

Received 14 April; accepted 8 June 2000.

1. Delovitch, T. & Singh, B. The nonobese diabetic mouse as a model of autoimmune diabetes: immune disregulation gets the NOD. *Immunity* **7,** 727–738 (1997).
2. Anderson, B., Park, B. J., Verdaguer, J., Amrani, A. & Santamaria, P. Prevalent $CD8^+$ T cell response against one peptide/MHC complex in autoimmune diabetes. *Proc. Natl Acad. Sci. USA* **96,** 9311–9316 (1999).
3. Nagata, M., Santamaria, P., Kawamura, T., Utsugi, T. & Yoon, J.-W. Evidence for the role of CD8+ cytotoxic T cells in the destruction of pancreatic beta cells in NOD mice. *J. Immunol.* **152,** 2042–2050 (1994).
4. Katz, J., Benoist, C. & Mathis, D. Major histocompatibility complex class I molecules are required for the generation of insulitis in non-obese diabetic mice. *Eur. J. Immunol.* **23,** 3358–3360 (1993).
5. Wicker, L. *et al.* β2-microglobulin-deficient NOD mice do not develop insulitis or diabetes. *Diabetes* **43,** 500–504 (1994).
6. Serreze, D., Leiter, E., Christianson, G., Greiner, D. & Roopenian, D. Major histocompatibility complex class I-deficient NOD.β1m^{null} mice are diabetes and insulitis resistant. *Diabetes* **43,** 505–508 (1994).
7. Verdaguer, J. *et al.* Acceleration of spontaneous diabetes in TCRβ-transgenic nonobese diabetic mice by beta cell-cytotoxic CD8+ T cells expressing identical endogenous TCRα chains. *J. Immunol.* **157,** 4726–4735 (1996).
8. Verdaguer, J. *et al.* Spontaneous autoimmune diabetes in monoclonal T cell nonobese diabetic mice. *J. Exp. Med.* **186,** 1663–1676 (1997).
9. DiLorenzo, T. *et al.* Major histocompatibility complex class I-restricted T cells are required for all but the end stages of diabetes development in nonobese diabetic mice and use prevalent T cell receptor α chain gene rearrangement. *Proc. Natl Acad. Sci. USA* **95,** 12538–12543 (1998).
10. Santamaria, P. *et al.* Beta cell cytotoxic CD8+ T cells from non-obese diabetic mice use highly homologous T cell receptor alpha chain CDR3 sequences. *J. Immunol.* **154,** 2494–2503 (1995).
11. Rammensee, H. G., Friede, T. & Stevanoviic, S. MHC ligands and peptide motifs: first listing. *Immunogenetics* **41,** 178–228 (1995).
12. Wong, S. *et al.* Identification of an MHC class I-restricted autoantigen in type 1 diabetes by screening an organ-specific cDNA library. *Nature Med.* **5,** 1026–1031 (1999).
13. Savage, P. A., Boniface, J. J. & Davis, M. M. A kinetic basis for T cell receptor repertoire selection during an immune response. *Immunity* **10,** 485-492 (1999).
14. Abiru, N. & Eisenbarth, G. Autoantibodies and autoantigens in type 1 diabetes: role in pathogenesis, prediction and prevention. *Can. J. Diab. Care* **23,** 59–65 (1999).
15. Kaufman, D. *et al.* Spontaneous loss of T-cell tolerance to glutamic acid decarboxylase in murine insulin-dependent diabetes. *Nature* **366,** 69–72 (1993).
16. Tisch, R. *et al.* Immune response to glutamic acid decarboxylase correlates with insulitis in non-obese diabetic mice. *Nature* **366,** 72–75 (1993).
17. Wegmann, D. The immune response to islet in experimental diabetes and insulin-dependent diabetes mellitus. *Curr. Opin. Immunol.* **8,** 860–864 (1996).
18. Alam, S. *et al.* T-cell receptor affinity and thymocyte positive selection. *Nature* **381,** 616–620 (1996).
19. Kersh, G., Kersh, E., Fremont, D. & Allen, P. High and low potency ligands with similar affinities for the TCR: the importance of kinetics in TCR signaling. *Immunity* **9,** 817–826 (1998).
20. Lyons, D. *et al.* A TCR binds to antagonist ligands with lower affinities and faster dissociation rates than to agonists. *Immunity* **5,** 53–61 (1996).
21. Matsui, K., Boniface, J., Steffner, P., Reay, P. & Davis, M. Kinetics of T-cell receptor binding to peptide/I-A^k complexes:correlation of the dissociation rate with T-cell responsiveness. *Proc. Natl Acad. Sci. USA* **91,** 12862–12866 (1994).
22. Monks, C., Freiberg, B., Kupfer, H., Sciaky, N. & Kupfer, A. Three dimensional segregation of supramolecular activation clusters in T-cells. *Nature* **395,** 82–86 (1998).
23. Reich, Z. *et al.* Ligand-specific oligomerization of T-cell receptor molecules. *Nature* **387,** 617–620 (1997).
24. Altman, J. *et al.* Direct visualization and phenotypic analysis of virus-specific T lymphocytes in HIV-infected individuals. *Science* **274,** 94–96 (1996).

Acknowledgements

The authors thank S. Bou, K. Rouleau, M. Deumas and S. Culp for animal care; S. Thiessen for scoring insulitis; M Bevan, K. Kane and T. Utsugi for reagents; S. Wong for testing the INS tetramer; Y. Yang for reading the manuscript; and H. Kominek for editorial assistance. This work was supported by grants from the Medical Research Council of Canada, the MRC/Juvenile Diabetes Foundation International (JDFI) Program II and the Canadian Diabetes Association (to P.S.). A.A. was supported by fellowships from the Alberta Heritage Foundation for Medical Research (AHFMR) and the JDFI. P.S. is a Senior Scholar of the AHFMR. R.T. and P.S. are members of the Beta Cell Apoptosis Network (BetaCAN).

Correspondence and requests for materials should be addressed to P.S. (e-mail: psantama@ucalgary.ca).

The Syk tyrosine kinase suppresses malignant growth of human breast cancer cells

Peter J. P. Coopman*†, Michael T. H. Do*, Mara Barth*, Emma T. Bowden‡, Andrew J. Hayes‡, Eugenia Basyuk§, Jan K. Blancato‖, Phyllis R. Vezza¶, Sandra W. McLeskey‡#, Paul H. Mangeat☆ & Susette C. Mueller*‡

*Departments of * Cell Biology, ‡ Oncology, ¶ Pathology, # Pharmacology and School of Nursing, ‖ Institute for Molecular and Human Genetics, and Vincent T. Lombardi Cancer Center, Georgetown University Medical School, Washington DC 20007, USA*
§ Centre National de la Recherche Scientifique UPR 9023 and ☆ Centre National de la Recherche Scientifique UMR 5539, 34095 Montpellier, France

Syk is a protein tyrosine kinase that is widely expressed in haematopoietic cells. It is involved in coupling activated immunoreceptors to downstream signalling events that mediate diverse cellular responses including proliferation, differentiation and phagocytosis[1–4]. Syk expression has been reported in cell lines of epithelial origin[5], but its function in these cells remains unknown. Here we show that Syk is commonly expressed in normal human breast tissue, benign breast lesions and low-tumorigenic breast cancer cell lines. Syk messenger RNA and protein, however, are low or undetectable in invasive breast carcinoma tissue and cell lines. Transfection of wild-type Syk into a Syk-negative breast cancer cell line markedly inhibited its tumour growth and metastasis formation in athymic mice. Conversely, overexpression of a kinase-deficient Syk in a Syk-positive breast cancer cell line significantly increased its tumour incidence and growth. Suppression of tumour growth by the reintroduction of Syk appeared to be the result of aberrant mitosis and cytokinesis. We propose that Syk is a potent modulator of epithelial cell growth and a potential tumour suppressor in human breast carcinomas.

To determine whether Syk has a role in breast cancer phagocytosis and invasion[6,7], we tested the expression of Syk in a panel of well-

† Present address: Centre National de la Recherche Scientifique UMR 5539, Montpellier, France.

characterized human breast cancer cell lines by polymerase chain reaction with reverse transcription (RT–PCR) (Fig. 1a, b). K562 erythroleukaemic cells, known to express Syk, were used as a positive control. Syk was expressed in normal human mammary gland tissue as well as in the human breast epithelium cell line MCF10A. It was also strongly expressed in several human breast carcinoma cell lines (MDA-MB-468, BT474, MCF7, SKBr3), but poorly expressed (Hs578T, MDA-MB-436) or undetectable in others (BT549, MDA-MB-231, MDA-MB-435). Nucleotide sequencing and Southern hybridization with an internal Syk probe (Fig. 1a, Syk-Biot.) proved that we had amplified Syk fragments. We detected Syk protein by immunoprecipitation and western blotting of cell extracts (Fig. 1c). Syk protein levels in the various breast cancer cell lines were comparable with those in the K562 cells. Corresponding to the absence of Syk mRNA, several breast cancer cell lines did not show any detectable Syk protein. Most strikingly, Syk was absent only in highly tumorigenic breast cancer cell lines displaying typical features of a malignant phenotype including increased motility and invasion[8] (Table 1). The ZAP-70 protein tyrosine kinase, which shares high amino-acid sequence homology with Syk[9], was not detected in the breast cancer cell lines (data not shown). These observations indicate that loss of Syk expression may be associated with the progression towards a malignant phenotype in breast cancer.

The Syk protein expressed by breast tumour cells was catalytically active (Fig. 1d). *In vitro*, Syk from MCF7 cells was autophosphorylated in an immunocomplex kinase assay. Treatment of cells with pervanadate, a phosphotyrosine phosphatase inhibitor, led to activation of Syk[10] and induced Syk autophosphorylation in

Table 1 Syk protein and mRNA expression in breast cancer cell lines

Breast cancer cell line	*In vivo* (*nu/nu*)*	Chemo-invasion†	Matrigel morphology‡	Syk RNA§	Syk protein‖
MDA-MB-231	LI	+++++	INV	–	–
BT549	N	+++++	INV	–	–
Hs578T	HM	+++++	INV	+/–	–
MCF7-ADR	P	+++	INV	n.d.	–
MDA-MB-435	LI	+++	INV	–	–
MDA-MB-436	LI	+++	INV	+/–	–
MCF7	P	++	SPH	+	+
BT474	P	+	SPH	+	+
MDA-MB-468	P	+	SPH	+	+
SKBr3	N	+	SPH	+	+
MCF10A	nd	nd	nd	+	+

*Activity in athymic nude mice: N, non-tumorigenic; P, primary tumour formation, no local invasiveness or metastasis; LI = local invasion through peritoneum, colonization of visceral organs; HM, hematogenous metastasis to the lungs; n.d., not determined. Data taken from ref. 8.
† Activity in Boyden chamber chemoinvasion assay. Data taken from ref. 8.
‡ Morphology in Matrigel: SPH, spherical colony or non-invasive cluster formation; INV, invasive colony formation. Data taken from ref. 8.
§ As determined by RT–PCR (see Fig. 1a, b).
‖ As determined by immunoprecipitation followed by western blotting (see Fig. 1c).

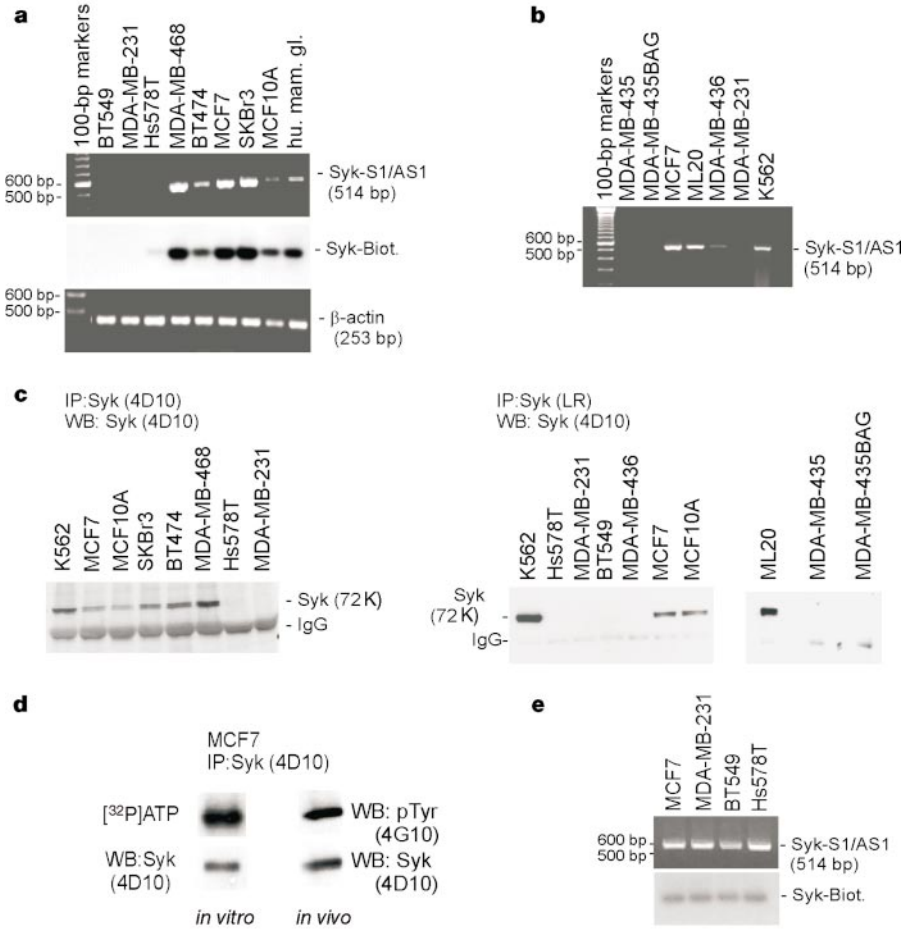

Figure 1 Syk expression in human breast cancer cell lines. **a**, RT–PCR detection of Syk and β-actin mRNA. Southern blotting of the RT–PCR products using a biotinylated internal Syk oligonucleotide (Syk-Biot.). hu. mam. gl., human mammary gland. **b**, RT–PCR detection of Syk mRNA in cell lines including the transfection acceptor cell lines ML20 and MDA-MB-435BAG and the K562 erythroleukaemia cell line. **c**, Immunoprecipitation (IP) and western blot (WB) detection of Syk protein using polyclonal (LR) and monoclonal (4D10) antibodies. **d**, Autophosphorylation activity of immunoprecipitated Syk as detected by *in vitro* incorporation of [γ-^{32}P]ATP or by western blotting with anti-phosphotyrosine (pTyr) antibodies. **e**, PCR and Southern blot detection of Syk in genomic DNA.

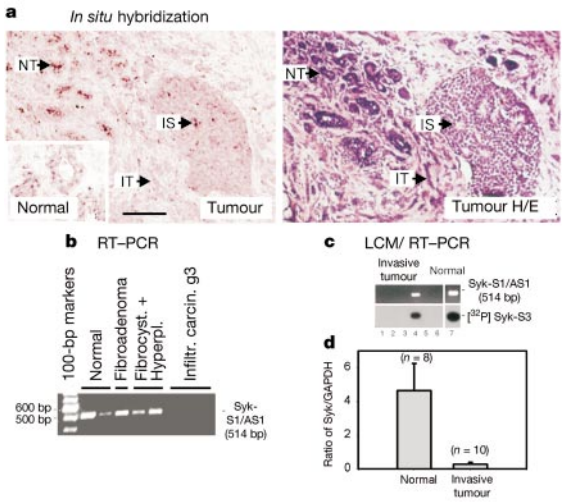

Figure 2 Syk expression in normal and pathological human breast tissue samples. **a**, *In situ* hybridization of Syk in normal breast tissue (NT), *in situ* tumour (IS) and invasive breast tumour (IT). H/E, haematoxylin and eosin stain. Scale bar, 500 μm; inset is enlarged twofold. **b**, RT–PCR detection of Syk mRNA in normal breast tissue, benign breast disease and grade 3 infiltrating breast carcinoma. **c**, RT–PCR detection of Syk in invasive breast carcinoma and normal breast tissue isolated by laser capture microdissection (LCM) (Syk-S1/AS1). Southern blotting of the RT–PCR products using an internal oligonucleotide (Syk-S3-[^{32}P]). **d**, [^{32}P]Syk-S3/ [^{32}P]GAPDH Southern blot signal ratios from LCM/RT–PCR breast tumour samples (Mean values ± s.e.).

MCF7 cells. The absence of Syk protein in malignant breast cancer cell lines does not seem to be caused by the previously reported frameshift mutation that generates a premature termination codon[11] as we did not detect Syk mRNA in these cells. PCR of genomic DNA demonstrated that the Syk gene is still present in all tested cell lines regardless of their Syk expression (Fig. 1e). Together, our results suggest that regulation of the Syk expression in breast cancer cell lines occurs at the transcriptional level; however, the exact mechanism of regulation is unknown.

As Syk expression is lost in malignant human breast cancer cell lines, we extended our study to normal and pathological human breast tissue samples. *In situ* hybridization verified that Syk expression in breast epithelial cells aligned within the ducts, whereas Syk expression was reduced in *in situ* carcinoma and lost in invasive breast carcinoma cells (Fig. 2a). Using RT–PCR, we detected Syk mRNA in normal breast tissue and in benign breast lesions (fibroadenoma, fibrocystic disease with hyperplasia), but not in malignant breast cancer (grade 3 infiltrating carcinoma) (Fig. 2b). Breast tumours are histologically and biochemically heterogeneous and might also contain normal breast epithelial cells or tumour-infiltrating lymphocytes that express Syk. To analyse Syk expression in invasive breast carcinoma cells or adjacent normal breast tissue exclusively, we used laser capture microdissection (LCM) followed by RT–PCR. Unlike normal breast tissue, most invasive tumour samples did not show any detectable Syk expression (Fig. 2c). Furthermore, Syk/GAPDH ratios in the LCM samples were significantly higher ($P < 0.01$, Student's t-test) in normal breast

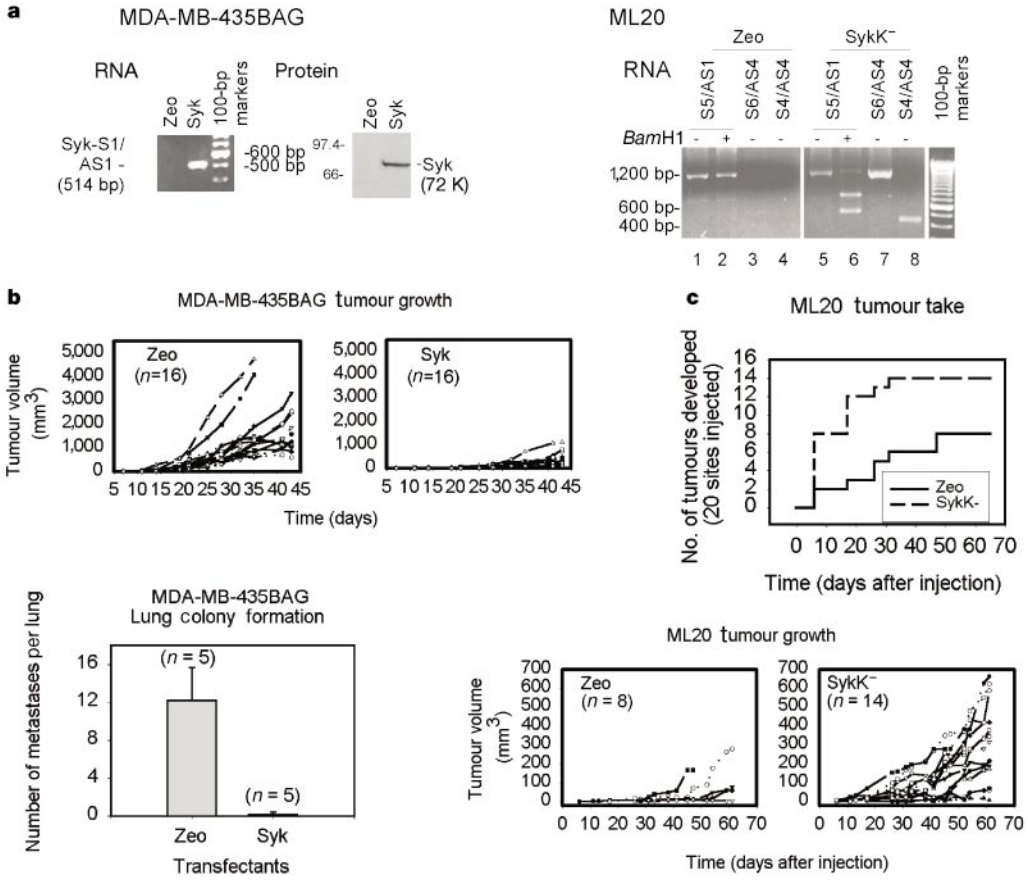

Figure 3 Effect of Syk transfection on tumorigenesis and metastasis formation *in vivo*. **a**, RT–PCR and western blot detection of wild-type Syk and kinase-negative Syk (SykK$^-$) expression in MDA-MB-435BAG and ML20 stable transfectants. The S4, S6 and AS4 primers specifically amplify mutant porcine Syk. The S5 and AS1 primers amplify both human and porcine Syk, but *Bam*H1 digests only mutated porcine Syk. **b**, Tumour growth and lung colony formation of wild-type Syk-transfected MDA-MB-435BAG cells in athymic mice. Lines represent growth of individual tumours. **c**, Tumour take and tumour growth of kinase-negative Syk-transfected ML20 cells in athymic ovariectomized mice, supplemented with a 17-β-oestradiol pellet. Lines represent growth of individual tumours.

epithelial cells as compared with invasive breast carcinoma cells (Fig. 2c). Our observations of cell lines and human tissue samples strongly suggest that Syk might block uncontrolled cell growth in normal breast tissue and that its absence may be permissive for malignant tumour growth.

We directly tested the effect of Syk transfection on tumorigenicity in an animal model. The use of *lacZ*-expressing acceptor cell lines allowed chromogenic detection of the transfected cells after injection in athymic mice. The Syk-negative MDA-MB-435BAG cells[12] were stably transfected with wild-type Syk complementary DNA. We verified Syk expression at both the mRNA (RT–PCR) and protein (western blotting) levels (Fig. 3a, MDA-MB-435BAG), and found that it was comparable to the endogeneous levels in MCF7 cells. The catalytic activity of the transfected Syk was validated by its *in vitro* autophosphorylation activity (data not shown). Conversely, Syk-positive ML20 cells[13], a variant of the MCF7 cell line, were transfected with a kinase-deficient mutant of porcine Syk (SykK$^-$) known to exert a dominant-negative function[14]. Its expression was specifically discriminated from the wild-type endogeneous human Syk by RT–PCR using porcine-specific Syk primers (Fig. 3a, ML20, lanes 7–8). Less stringent primers amplified both human and porcine Syk, but a *Bam*H1 digest allowed specific detection of the point mutation introduced into the kinase-deficient porcine Syk. This approach showed that the dominant-negative Syk is expressed at higher levels than the wild-type Syk in ML20/SykK$^-$ transfectants (Fig. 3a, ML20, lane 6, compare faint upper band with lower two bands). Expression of the kinase-deficient Syk did not, however, alter the protein levels of the endogeneous wild-type Syk in ML20/SykK$^-$ transfectants (data not shown).

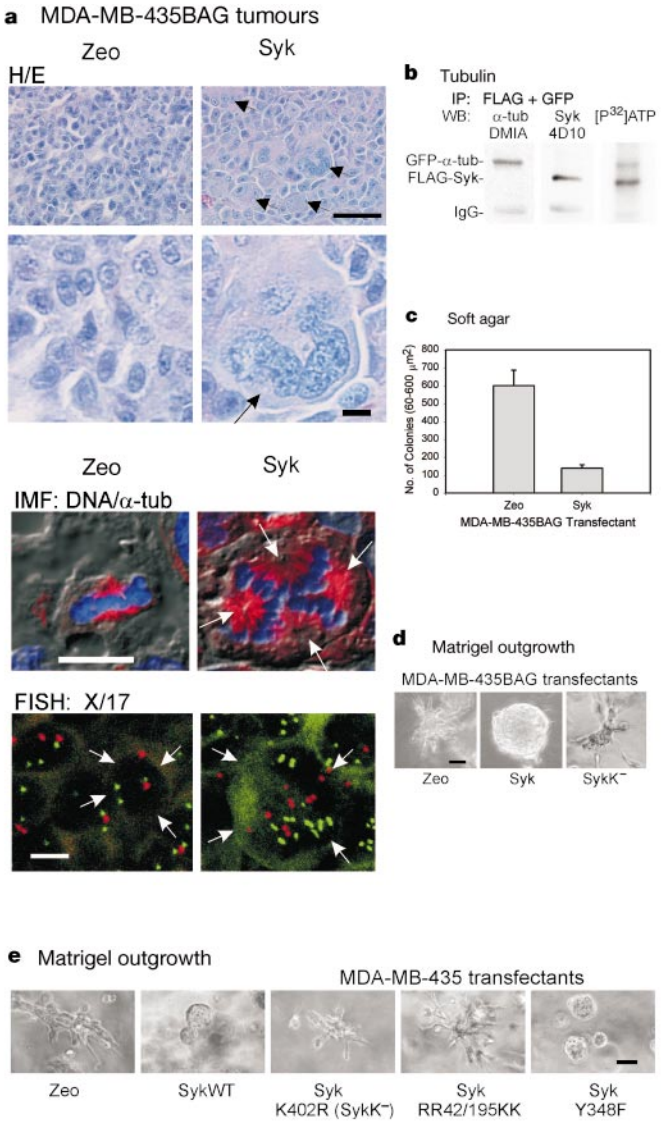

Figure 4 Biological consequences of Syk transfection in MDA-MB-435 cells. **a**, Paraffin sections of experimentally induced tumours stained with haematoxylin/eosin (H/E), anti-α-tubulin (red) and ToPro3 (DNA, blue) and FISH for chromosomes 17 (red) and X (green). Arrows indicate enlarged cells (in H/E), spindle poles (in IMF) or margins of individual cells (in FISH). Scale bars are 5 μm except in low-magnifcation H/E stains (20 μm). **b**, Phosphorylation of α-tubulin by Syk in an immunocomplex kinase assay with epitope-tagged proteins in Cos1 cells. **c**, Anchorage-independent cell growth (mean ± s.e.). **d**, **e**, Outgrowth in Matrigel of cells transfected with wild-type or mutated Syk. Scale bar, 100 μm.

Immediately after selection in zeocin, we injected the pooled transfected clones into the mammary fat pad of female athymic mice. All MDA-MB-435BAG tumours, regardless of the transfection, were already palpable 7 days after injection. Subsequently, the tumours of the MDA-MB-435BAG/Zeo control transfectants grew steadily, attaining mean volumes of 2,004 ± 1,158 mm^3 (mean ± s.d.) after 35 to 43 days (Fig. 3b). In contrast, the tumour growth of the Syk transfectants was significantly slower than that of the control transfectants ($P < 0.005$, Fisher variance analysis). At sacrifice (day 43), the Syk tumours reached a mean volume of only 419 ± 297 mm^3, which was significantly smaller than the control (Zeo) tumours ($P < 0.001$, Student's *t*-test). Mammary-fat-pad-injected MDA-MB-435BAG transfectants did not develop any detectable spontaneous metastases after 43 days. We therefore tested their capacity to form experimental lung metastases after injection in the tail vein. With the Syk transfectants, only one of five animals showed a single metastatic colony in the lungs (Fig. 3b). In contrast, all animals injected with control (Zeo) cells developed several metastatic lung colonies. These results clearly show that re-expression of Syk by MDA-MB-435BAG cells was sufficient to suppress their tumour growth and metastasis formation. The latency period for tumour appearance of the mammary-fat-pad-injected ML20 transfectants was very variable and ranged from 6 to 47 days, regardless of the transfection (Fig. 3c). The potency of the SykK$^-$ transfectants to develop a tumour (tumour take), however, was significantly increased as compared with the control (Zeo) transfectants ($P < 0.001$, Student's *t*-test). In addition, the overall tumour growth of the SykK$^-$ transfectants was significantly faster than that of the control transfectants ($P < 0.005$, Fisher variance analysis) (Fig. 3c). We conclude that expression of the dominant-negative, kinase-deficient Syk releases growth inhibition in MCF7 cells that is dependent upon Syk tyrosine kinase activity.

To investigate the mechanisms underlying the suppressive effect of Syk expression on tumour growth, we studied apoptosis by *in situ* TUNEL (terminal deoxyribonucleotide transferase (TdT)-mediated dUTP nick end labelling) staining of histological sections of the primary tumours of MDA-MB-435BAG transfectants. The number of apoptotic nuclei per square micrometre was determined for tumour sections exclusive of necrotic areas, 6.38 ± 6.58 (Zeo, $n = 11$) and 5.49 ± 2.32 (Syk, $n = 7$), and exhibited no significant statistical difference (Student's *t*-test). Therefore, programmed cell death does not seem to account for the inhibited tumour growth; however, staining of the MDA-MB-435BAG tumour sections with haematoxylin and eosin highlighted abnormalities in cell division. Unlike control (Zeo) tumours, Syk tumours exhibited groups of three to many cells that were enlarged with multilobed or multiple nuclei (Fig. 4a, H/E). In addition, spindles surrounding metaphase chromosomes were abnormal, displaying multiple spindle poles and conflicting attachments to condensed chromosomes (Fig. 4a, DNA/α-tub). Fluorescent *in situ* hybridization (FISH) enumeration of chromosome X and 17 centromeres showed that the enlarged cells were hyperdiploid, that is, having more than the normal number of chromosomes X and 17 (Fig. 4a, X/17). Therefore, we

propose that tumour growth is blocked after abnormal mitosis and failure of subsequent cytokinesis in cells transfected with Syk. We showed that α-tubulin is phosphorylated by Syk in an immunocomplex kinase assay *in vitro* (Fig. 4b). α-Tubulin is also an *in vivo* substrate for Syk in activated B cells[15]. Moreover, it is phosphorylated on a tyrosine residue in the carboxy-terminal region containing the sites of interaction with the microtubule-associated proteins that regulate microtubule assembly and function[15]. Syk might therefore alter the microtubule/tubulin monomer equilibrium and ultimately affect mitosis. In agreement with our observations, abnormal mitoses due to altered microtubule organization have been observed in breast tumours[16].

In vitro, all MDA-MB-435BAG transfectants showed an indistinguishable logarithmic proliferation on plastic substratum (data not shown); however, the MDA-MB-435BAG/Syk cells displayed a significantly decreased ability to grow in anchorage-independent conditions as compared to the control (Zeo) transfectants ($P < 0.005$, Student's *t*-test) (Fig. 4c). We observed that the ability of breast cancer cell lines to form invasive colonies in Matrigel, a naturally occurring basement membrane matrix, was inversely correlated with their Syk expression (Table 1; ref. 8). Correspondingly, all MDA-MB-435BAG/Zeo colonies displayed an invasive morphology with single cells penetrating the surrounding Matrigel matrix (Fig. 4d). The Syk-expressing colonies, in contrast, exhibited a well-delineated, non-invasive spherical appearance. Stable expression of a kinase-negative Syk ($SykK^-$) by these cells was not sufficient to suppress invasive outgrowth.

In summary, Syk expression specifically inhibits anchorage-independent proliferation and abates extracellular matrix invasion *in vitro*. As biological effects with Syk-transfected cells were only observed in animal experiments and in Matrigel but not on plastic substratum, we propose that the extracellular matrix might contain the signals that activate Syk[17]. We then generated several FLAG-tagged Syk mutants and tested their effect on Matrigel outgrowth after stable transfection in the Syk-negative MDA-MB-435 cells (Fig. 4e). Mutant Syk proteins with functionally inactive SH2 domains (RR42/195KK)[18] or lacking kinase activity (K402R) lost their capacity to suppress the invasive outgrowth of cells in Matrigel. However, it was ineffective to mutate an autophosphorylated tyrosine residue in the Syk linker region (Y348F) that is critical for its interaction with the Vav[19] and the PLC-γ1 SH2 domains[20]. This suggests that other Syk effectors may be necessary for the suppression of invasive outgrowth in Matrigel.

In conclusion, we have shown that the Syk tyrosine kinase is commonly expressed by normal breast epithelial cells, that loss of Syk expression is associated with the acquisition of a malignant breast tumour phenotype, and that Syk may directly act as a tumour suppressor, presumably by controlling cell division. We therefore propose that loss of Syk expression may function with other genetic alterations in the multistep process of breast tumour development and progression. This negative correlation is unexpected when considered with the current concept that tyrosine kinases are positively associated with tumorigenesis (for example, c-erbB2). Interestingly, allelic loss on chromosome 9q22, the human Syk locus, has been reported to be associated with lymph node metastasis of primary breast cancer[21]. As Syk knockout mice die perinatally, the effects of loss of Syk expression on breast development have not been not observed[22,23], but knockout mice lacking c-Cbl, a regulator of Syk, develop mammary epithelial hyperplasia[24]. □

Methods

Cells lines and tissue samples

The MCF10A and K562 cell lines were obtained from the ATCC (Manassas, VA). All other human breast cancer cell lines were provided by the Tissue Culture Shared Resources of the Lombardi Cancer Center. Human tissue samples were obtained from the Cooperative Human Tissue Network (Univ. Pennsylvania, Philadelphia), the Lombardi Cancer Center Histopathology and Tissue shared resource, and C. Theillet (CNRS UMR 5535, CRLC Val d'Aurelle, Montpellier, France). Human mammary gland total RNA was purchased from Clontech.

Immunoprecipitation, western blotting and *in vitro* kinase activity

Cells were lysed as described[6]. Syk was immunoprecipitated and detected on nitrocellulose membrane by western blotting with commercial antibodies (Santa Cruz Biotechnology) and enhanced chemiluminescence (Amersham Pharmacia). The following antibodies were used: mouse monoclonal anti-phosphotyrosine (4G10; UBI, Lake Placid, NY), anti-α-tubulin (DMIA; Neomarkers, Fremont, CA), anti-FLAG antibody (M2; Sigma) and the rabbit polyclonal anti-GFP (Torrey Pines Biolabs, San Diego, CA). The autophosphorylation capacity of immunoprecipitated Syk was evaluated by the *in vitro* incorporation of 10 μCi [γ-^{32}P]ATP. Pervanadate (1 mM Na_3VO_4 + 1 mM H_2O_2) treatment of cells was carried out for 15 min at 37 °C.

PCR and Southern hybridization

The following human Syk primers were used for RT–PCR and genomic PCR: Syk-S1 forward, 5′-CATGTCAAGGATAAGAACATCATAGA-3′; Syk-S3 forward, 5′-GTGTTGCTAGTTACCCAACATTACGC-3′; Syk-S5 forward, 5′-AAAGAAGTTCGACACGCTCTGG-3′; and Syk-AS1 reverse, 5′-AGTTCACCACGTCATAGTAGTAATT-3′. Primers amplifying specifically porcine Syk were Syk-S4 forward, 5′-TGGGCAAACGGGAAATGATA-3′; Syk-S6 forward, 5′-TGTCAGGAGAAGGCGCAGG-3′; and Syk-AS4 reverse, 5′-ATTGGCCTCATTTTTCAGGATCC-3′. Human β-actin primers correspond to nucleotides 936–955 (forward) and 1170–1189 (reverse). Human GAPDH primers correspond to nucleotides 67–86 (forward), 504–523 (reverse) and 361–380 (internal oligonucleotide). Southern hybridization was performed on Nylon membrane and Syk was detected with a biotinylated internal oligonucleotide (Syk–Biot., 5′-AGTTGATGCATTCCG GAGCG-3′). For Southern hybridization of LCM/RT–PCR samples, internal primers were radiolabelled with [^{32}P]dATP using T4 polynucleotide kinase.

In situ hybridization

A 140-bp nucleotide fragment of the human Syk cDNA (nucleotides 472–611) was subcloned into the pGEM9Zf vector (Promega) and used to generate digoxigenin-UTP labelled cRNA probes by *in vitro* transcription. *In situ* hybridization was performed as described[25] and the signal revealed with alkaline phosphatase and NBT/BCIP substrate (Boehringer). A *lacZ* non-sense probe was used as negative control.

Laser capture microdissection (LCM)

Laser microdissection of a 30 μm diameter capture area was done as described[26] using a Pixcell LCM system (Arcturus Engineering, Mountain View, California). Total RNA was retrieved and used for RT–PCR.

Vector construction and mutagenesis

The wild-type human Syk cDNA and the mutated kinase-deficient porcine Syk cDNA (K395R) were respectively provided by S. Yagi (Tonen Corp. Res. Dev. Lab., Saitama, Japan)[27] and T. Kurosaki (Kansai Medical Univ., Moriguchi, Japan)[14]. Both cDNAs were recloned into the pcDNA3.1-Zeo (+) mammalian expression vector (Invitrogen), verified by sequencing and transfected using electroporation. After selection in Zeocin (800 μg ml^{-1}), 10–50 stably transfected clones were obtained and pooled to avoid unrepresentative subcloning artefacts. Alternatively, the human Syk coding sequence was amplified by PCR and cloned into the pCAF1 expression vector (gift of P. Burbelo, Georgetown Univ. Medical Center, Washington DC) to encode an amino-terminal FLAG-tagged Syk. Point mutations in the Syk coding sequence were generated (QuickChange, Stratagene) and verified by sequencing. Mutant Syk cDNAs were stably transfected using SuperFect reagent (Qiagen) and selected in G418 (800 μg ml^{-1}) and their expression and catalytic activity were verified. The pEGFP–α-tubulin vector was purchased from Clontech.

Animal experiments

To determine their tumorigenicity, cells were injected subcutaneously (two to five million cells) into the mammary fat pad of 4–6-week-old female NCr *nu/nu* mice that were intact or ovariectomized and supplemented with a subcutaneously implanted 17-β-oestradiol pellet (Innovative Research, Rockville, Maryland)[8]. Primary tumours and organs (lungs, liver, spleen, lymph nodes) were fixed or snap frozen for immunohistochemistry or whole organ X-gal staining[12]. To determine their metastatic capacity, two million cells were injected into the tail vein. After 4 weeks, the number of lung colonies were counted using a dissecting microscope and histologically confirmed.

TUNEL, immunohistochemistry and FISH

Apoptosis was detected by TUNEL using the TACS 2 TdT kit (Trevigen, Gaithersburg, Maryland) and quantified using Optimas 5.2 image analysis software[6] (Bothell, Washington). α-Tubulin was visualized using monoclonal mouse-anti-α-tubulin antibodies (clone B-5-1-2; Sigma) followed by Texas Red anti-mouse (Jackson Laboratories) and counterstained for DNA using ToPro3 (Molecular Probes). FISH for chromosomes 17 and X was done using directly labelled centromeric probes (Vysis, Downers Grove, Illinois)[28].

In vitro assays

Anchorage-independent growth in soft agar was carried out in triplicate as described[29] and counted with an Omnicron 3800 tumour colony analyser (Imaging Products International, Chantilly, Virginia). Matrigel outgrowth was assessed as described[8] and observed on a Zeiss IM35 inverted microscope.

Received 17 February; accepted 24 May 2000.

1. Cheng, A. M. & Chan, A. C. Protein tyrosine kinases in thymocyte development. *Curr. Opin. Immunol.* **9,** 528–533 (1997).
2. Kurosaki, T. Molecular mechanisms in B cell antigen receptor signaling. *Curr. Opin. Immunol.* **9,** 309–318 (1997).
3. Chu, D. H., Morita, C. T. & Weiss, A. The Syk family of protein tyrosine kinases in T-cell activation and development. *Immunol. Rev.* **165,** 167–180 (1998).
4. Indik, Z. K., Park, J. G., Pan, X. Q. & Schreiber, A. D. Induction of phagocytosis by a protein tyrosine kinase. *Blood* **85,** 1175–1180 (1995).
5. Fluck, M., Zurcher, G., Andres, A. C. & Ziemiecki, A. Molecular characterization of the murine Syk protein tyrosine kinase cDNA, transcripts and protein. *Biochem. Biophys. Res. Commun.* **213,** 273–281 (1995).
6. Coopman, P. J., Do, M. T. H., Thompson, E. W. & Mueller, S. C. Phagocytosis of cross-linked gelatin matrix by human breast carcinoma cells correlates with their invasive capacity. *Clin. Canc. Res.* **4,** 507–515 (1998).
7. Coopman, P. J., Thomas, D. M., Gehlsen, K. R. & Mueller, S. C. Integrin α3β1 participates in the phagocytosis of extracellular matrix molecules by human breast cancer cells. *Mol. Biol. Cell* **7,** 1789–1804 (1996).
8. Thompson, E. W. *et al.* Association of increased basement membrane invasiveness with absence of estrogen receptor and expression of vimentin in human breast cancer cell lines. *J. Cell Physiol.* **150,** 534–544 (1992).
9. Law, C. L. *et al.* Molecular cloning of human Syk. A B cell protein-tyrosine kinase associated with the surface immunoglobulin M-B cell receptor complex. *J. Biol. Chem.* **269,** 12310–12319 (1994).
10. Nagai, K., Inazu, T. & Yamamura, H. p72syk is activated by vanadate plus H_2O_2 in porcine platelets and phosphorylates GTPase activating protein on tyrosine residue(s). *J. Biochem. (Tokyo)* **116,** 1176–1181 (1994).
11. Fargnoli, J. *et al.* Syk mutation in Jurkat E6-derived clones results in lack of $p72^{syk}$ expression. *J. Biol. Chem.* **270,** 26533–26537 (1995).
12. Brunner, N. *et al. lacZ* transduced human breast cancer xenografts as an *in vivo* model for the study of invasion and metastasis. *Eur. J. Cancer* **28A,** 1989–1995 (1992).
13. Kurebayashi, J. *et al.* Quantitative demonstration of spontaneous metastasis by MCF-7 human breast cancer cells cotransfected with fibroblast growth factor 4 and *LacZ*. *Cancer Res.* **53,** 2178–2187 (1993).
14. Takata, M. *et al.* Tyrosine kinases Lyn and Syk regulate B cell receptor-coupled Ca^{2+} mobilization through distinct pathways. *EMBO J.* **13,** 1341–1349 (1994).
15. Peters, J. D., Furlong, M. T., Asai, D. J., Harrison, M. L. & Geahlen, R. L. Syk, activated by cross-linking the B-cell antigen receptor, localizes to the cytosol where it interacts with and phosphorylates alpha-tubulin on tyrosine. *J. Biol. Chem.* **271,** 4755–4762 (1996).
16. Lingle, W. L. & Salisbury, J. L. Altered centrosome structure is associated with abnormal mitoses in human breast tumors. *Am. J. Pathol.* **155,** 1941–1951 (1999).
17. Miranti, C. K., Leng, L., Maschberger, P., Brugge, J. S. & Shattil, S. J. Identification of a novel integrin signaling pathway involving the kinase Syk and the guanine nucleotide exchange factor Vav1. *Curr. Biol.* **8,** 1289–1299 (1998).
18. Williams, S. *et al.* Reconstitution of T cell antigen receptor-induced Erk2 kinase activation in Lck-negative JCaM1 cells by Syk. *Eur. J. Biochem.* **245,** 84–90 (1997).
19. Deckert, M., Tartare-Deckert, S., Couture, C., Mustelin, T. & Altman, A. Functional and physical interactions of Syk family kinases with the Vav proto-oncogene product. *Immunity* **5,** 591–604 (1996).
20. Law, C. L., Chandran, K. A., Sidorenko, S. P. & Clark, E. A. Phospholipase C-gamma1 interacts with conserved phosphotyrosyl residues in the linker region of Syk and is a substrate for Syk. *Mol. Cell. Biol.* **16,** 1305–1315 (1996).
21. Minobe, K. *et al.* Allelic loss on chromosome 9q is associated with lymph node metastasis of primary breast cancer. *Jpn. J. Cancer Res.* **89,** 916–922 (1998).
22. Turner, M. *et al.* Perinatal lethality and blocked B-cell development in mice lacking the tyrosine kinase Syk. *Nature* **378,** 298–302 (1995).
23. Cheng, A. M. *et al.* Syk tyrosine kinase required for mouse viability and B-cell development. *Nature* **378,** 303–306 (1995).
24. Murphy, M. A. *et al.* Tissue hyperplasia and enhanced T-cell signalling via ZAP-70 in c-Cbl- deficient mice. *Mol. Cell Biol.* **18,** 4872–4882 (1998).
25. Schaeren-Wiemers, N. & Gerfin-Moser, A. A single protocol to detect transcripts of various types and expression levels in neural tissue and cultured cells: in situ hybridization using digoxigenin-labelled cRNA probes. *Histochemistry* **100,** 431–440 (1993).
26. Emmert-Buck, M. R. *et al.* Laser capture microdissection. *Science* **274,** 998–1001 (1996).
27. Yagi, S., Suzuki, K., Hasegawa, A., Okumura, K. & Ra, C. Cloning of the cDNA for the deleted Syk kinase homologous to Zap- 70 from human basophilic leukemia cell line (KU812). *Biochem. Biophys. Res. Commun.* **200,** 28–34 (1994).
28. Pinkel, D. *et al.* Cytogenetic analysis by in situ hybridization with fluorescently labeled nucleic acid probes. *Cold Spring Harbor Symp. Quant. Biol.* **51,** 151–157 (1986).
29. Fang, W., Hartmann, N., Chow, D. T., Riegel, A. T. & Wellstein, A. Pleiotrophin stimulates fibroblasts and endothelial and epithelial cells and is expressed in human cancer. *J. Biol. Chem.* **267,** 25889–25897 (1992).

Acknowledgements

We gratefully acknowledge S. Yagi and T. Kurosaki who have provided the Syk cDNAs. We thank P. Burbelo for the pCAF1 vector; F. Kern for ML20 cells; J. Zwiebel for MDA-MB-435BAG cells; C. Theillet for tumour samples; A. Wright, F. Onajafe and M. Dai for technical assistance; S. Artero for statistics; and B. Singh and P. Roger for pathology advice. We also thank J. Brugge, N. Taylor, A. Wellstein and M. Lippman for comments on the manuscript. This work was supported in part by NIH grants (to S.C.M. and S.W.M.) and, in part, by the Lombardi Cancer Center shared resources supported by a US Public Health Service Grant.

Correspondence and requests for materials should be addressed to S.C.M. (e-mail: muellers@gunet.georgetown.edu).

Molecular portraits of human breast tumours

Charles M. Perou*†, Therese Sørlie†‡, Michael B. Eisen*, Matt van de Rijn§, Stefanie S. Jeffrey‖, Christian A. Rees*, Jonathan R. Pollack¶, Douglas T. Ross¶, Hilde Johnsen‡, Lars A. Akslen#, Øystein Fluge☆, Alexander Pergamenschikov*, Cheryl Williams*, Shirley X. Zhu§, Per E. Lønning, Anne-Lise Børresen-Dale‡, Patrick O. Brown¶†† & David Botstein***

** Department of Genetics, Stanford University School of Medicine, Stanford, California 94305, USA*
‡ Department of Genetics, The Norwegian Radium Hospital, N-0310 Montebello Oslo, Norway
§ Department of Pathology, Stanford University School of Medicine, Stanford, California 94305, USA
‖ Department of Surgery, Stanford University School of Medicine, Stanford, California 94305, USA
¶ Department of Biochemistry, Stanford University School of Medicine, Stanford, California 94305, USA
 # Department of Pathology, The Gade Institute, Haukeland University Hospital, N-5021 Bergen, Norway
☆ Department of Molecular Biology, University of Bergen, N-5020 Bergen, Norway
*** Department of Oncology, Haukeland University Hospital, N-5021 Bergen, Norway*
†† Howard Hughes Medical Institute, Stanford University School of Medicine, Stanford, California 94305, USA
† These authors contributed equally to this work

Human breast tumours are diverse in their natural history and in their responsiveness to treatments[1]. Variation in transcriptional programs accounts for much of the biological diversity of human cells and tumours. In each cell, signal transduction and regulatory systems transduce information from the cell's identity to its environmental status, thereby controlling the level of expression of every gene in the genome. Here we have characterized variation in gene expression patterns in a set of 65 surgical specimens of human breast tumours from 42 different individuals, using complementary DNA microarrays representing 8,102 human genes. These patterns provided a distinctive molecular portrait of each tumour. Twenty of the tumours were sampled twice, before and after a 16-week course of doxorubicin chemotherapy, and two tumours were paired with a lymph node metastasis from the same patient. Gene expression patterns in two tumour samples from the same individual were almost always more similar to each other than either was to any other sample. Sets of co-expressed genes were identified for which variation in messenger RNA levels could be related to specific features of physiological variation. The tumours could be classified into subtypes distinguished by pervasive differences in their gene expression patterns.

We proposed that the phenotypic diversity of breast tumours might be accompanied by a corresponding diversity in gene expression patterns that we could capture using cDNA microarrays. Systematic investigation of gene expression patterns in human breast tumours might then provide the basis for an improved molecular taxonomy of breast cancers. We analysed gene expression patterns in grossly dissected normal or malignant human breast tissues from 42 individuals (36 infiltrating ductal carcinomas, 2 lobular carcinomas, 1 ductal carcinoma *in situ*, 1 fibroadenoma and 3 normal breast samples). Fluorescently labelled (Cy5) cDNA was prepared from mRNA from each experimental sample. We prepared cDNA, labelled using a second distinguishable fluorescent nucleotide (Cy3), from a pool of mRNAs isolated from 11 different